

# Impact of Transmit Power Control on Aggregate Interference in Underlay Cognitive Radio Networks

Sachitha Kusaladharma, Prasanna Herath and Chintha Tellambura, *Fellow, IEEE*

Department of Electrical and Computer Engineering

University of Alberta, Edmonton, Alberta T6G 2V4, Canada

Email: {kusaladh,prasanna}@ualberta.ca and chintha@ece.ualberta.ca

**Abstract**—This paper analyzes how transmit power control affects the aggregate interference arising from a Poisson field of underlay cognitive radio (CR) transmitter nodes distributed in a finite area. We consider three per-user, location dependent power control schemes, when each CR transmitter is associated with the nearest CR receiver, where the CR receivers form a Poisson field in the entire 2-dimensional space. The 3 schemes are based on: 1) CR transmitter-receiver distance  $r_c$  2)  $r_c$  and a constant cut-off power level 3)  $r_c$  and a random cut-off power level, respectively. For each of these, the exact moment generating function (MGF) and mean of aggregate interference power are derived. We also investigate the primary system outage due to aggregate interference. Rayleigh fading and exponential path loss links are assumed. Monte-Carlo simulation results validate our analysis and also show that the CR power thresholds and node densities significantly affect the aggregate interference.

## I. INTRODUCTION

To improve power efficiency and lower co-channel interference, transmit power control is essential in modern wireless networks [1]. Power control methods can be categorized into fixed power, distance based, and measurement based schemes [2]. For example, open-loop and closed-loop power control schemes are used in Wideband Code Division Multiple Access (WCDMA) and Long Term Evolution (LTE) networks [1]. Transmit power controlling schemes have been widely studied in the literature [3]–[6], and their use in cognitive radio (CR) networks [7], [8] has also received attention [5], [6].

CR allows secondary users to opportunistically access pre-allocated spectrum. With regards to CR, underlay networks allow both primary and secondary networks to transmit simultaneously [7], [9]. However, since concurrent cognitive transmissions cause additional primary receiver (PR) interference, the resulting performance degradation must be kept below an acceptable level. This goal may be achieved by using transmit power thresholds for the CR transmitters (CRTs) or by imposing an exclusion region around the PR. To characterize the primary performance in such networks, the statistical properties of the aggregate interference are needed. In practical networks, the interference statistics depend on the locations and numbers of CR nodes, channel impairments, and transmit power control scheme in use. This paper takes all these into consideration, and investigates the aggregate interference as well as the performance of the primary system under 3 transmit power control schemes.

## A. Prior Research

Aggregate interference of cognitive networks has been extensively analyzed recently. While some works develop statistical interference models, others provide exact analysis and performance bounds. For example, [10] provides a statistical aggregate interference model considering path loss, small scale fading, shadowing, sensing techniques, and also investigates the effects of primary network transmit power control. On the other hand, [11] derives the moment generating function (MGF) and cumulants for underlay aggregate interference for distinct path loss exponents. A normal and log-normal sum approximation to the aggregate interference is developed in [12], while [13] approximates it with the nearest neighbor's interference. Considering intra-cognitive user interference, the average aggregate interference have been derived in [14]. The MGF of the aggregate interference for an underlay CR network was analyzed, and an approximation for it was proposed in [15] while considering the effects of shadowing. Moreover, [16] investigates the effects of different parameters (exclusion zone radius, numbers of CR nodes) for CR deployment under interference constraints to the primary system, whereas [17] analyses the probability density function (PDF) of the interference under different exclusion regions.

## B. Motivation and contribution

The primary objective of this paper is to provide an exact analysis of the aggregate interference for a finite area underlay CR network with three distinct transmit power control schemes. Previous research [11], [14], [16] has assumed constant CR transmit powers. While this assumption makes the system analytically tractable, in reality, the transmit powers depend on several factors including the distance to the intended CR receiver (CRR), and the maximum allowable transmit power. Reference [18] has provided pioneering research by considering a distance based power control scheme, and contention control scheme where active transmitters are modeled by a Matern-hardcore process, to limit the intra-cognitive interference. However, [18] does not provide an exact analysis.

We derive the MGF and mean of the aggregate interference for three CR transmit power control schemes, which are based on: 1) CR transmitter-receiver distance  $r_c$  2)  $r_c$  and a constant cut-off power level 3)  $r_c$  and a random cut-off power level. Moreover, the resulting outage probability of the PR is analyzed. The spatial distributions of the CRTs and CRRs

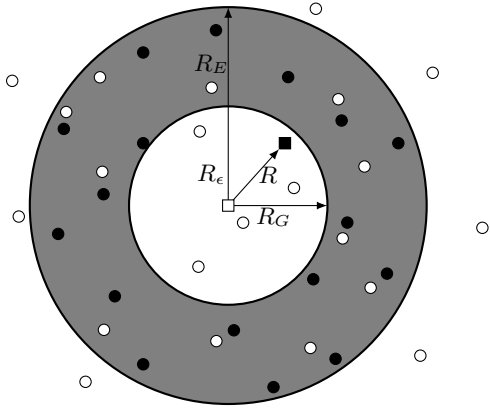


Fig. 1: System model. The CRTs are limited to the shaded area, while the CRRs are distributed in the entire 2-dimensional space. Respectively,  $R_G$ ,  $R_E$ , and  $R$  denote the guard distance, the outer distance, and the primary transmitter-receiver distance. Legend: black dot - CRT, white dot - CRR, white square - PR, black square - primary transmitter.

are characterized by two independent homogeneous Poisson point processes (PPPs) [19]. The CRTs are distributed over a finite annular region, with an exclusion zone surrounding the primary receiver (Fig. 1). The signals undergo exponential path-loss and Rayleigh fading.

This paper is organized as follows. Section II introduces the spatial and signal models. Section III derives the MGF and mean of the aggregate interference under the 3 power control schemes, while Section IV derives the outage probability of the PR. Section V provides numerical results, and Section VI concludes the paper.

**Notations:**  $\Gamma(x, a) = \int_a^\infty t^{x-1} e^{-t} dt$  and  $\Gamma(x) = \Gamma(x, 0)$  [20].  $\Pr[A]$  is the probability of event  $A$ ,  $f_X(\cdot)$  is the PDF,  $F_X(\cdot)$  is the cumulative distribution function (CDF),  $M_X(\cdot)$  is the MGF, and  $E_X[\cdot]$  denotes the expectation over random variable  $X$ .

## II. SYSTEM MODEL

This section introduces both the spatial and signal models.

### A. Spatial model

In the system model, without loss of generality, the PR is located at the center, and the primary transmitter is at a distance  $R$  from it. The CRTs are located in a finite annular area centered around the PR (Fig. 1). The exclusion (guard) zone where no CR transmissions take place has a radius  $R_G$ . This exclusion region plays an important role in underlay networks to limit the PR interference [11]. The interference from CRTs beyond the outer radius  $R_E$  is considered to be negligible due to path-loss. A field of CRTs distributed in the entire 2-dimensional plane is a special case of our model when  $R_G \rightarrow 0$  and  $R_E \rightarrow \infty$ . Conversely, the CRRs can be located within the exclusion region, and beyond  $R_E$ . Because the number and locations of CRTs and CRRs are random, they have to be modeled by a spatial stochastic process [21], [22]. In this paper, we characterize the spatial distribution of CRTs

and CRRs by independent homogeneous PPPs with intensities  $\lambda_t$  and  $\lambda_r$ , respectively. The PPP has extensively been used to characterize the spatial distribution of cognitive radio nodes in prior research [10], [11], [18]. According to the PPP model, the probability of having  $n$  nodes (transmitters or receivers) in a finite area  $A$  is given by [23],

$$P(n) = \frac{(\lambda_j A)^n}{n!} e^{-\lambda_j A}, \quad n = 0, 1, 2, \dots, \quad (1)$$

where  $j = \{r, t\}$ . In the subsequent analysis, we assume that all the CRTs transmit simultaneously. However, this assumption leads to a worst case scenario in terms of aggregate interference on the PR. Thus, our analysis reveals the maximum primary interference level. Nevertheless, there is no loss of generality in this assumption. Because each CRT only transmits independently with probability  $\beta$ , by using the Coloring theorem [19], our derived expressions can be adapted to quantify the performance of the networks by replacing  $\lambda_t$  with  $\beta\lambda_t$ . Furthermore, we will assume that each CRT is connected to the nearest CRR. Practical applications for such a network can include ad-hoc networks, wireless sensor networks, and cellular networks [24].

### B. Signal model

The interfering signals undergo path-loss and Rayleigh fading. For path-loss, the simplified path-loss model [25] is assumed. Therefore, the received power at a distance  $r$  from the transmitter is given by  $P_r = P_t r^{-\alpha}$ , where  $\alpha$  is the path-loss exponent, and  $P = P_0 r_0^\alpha$  is termed the power level.  $P_0$  is the received power at a distance of  $r_0$  in the far-field. For Rayleigh fading, the PDF of the  $i$ -th channel power gain is given by  $f_{|h_i|^2}(x) = e^{-x}$ ,  $0 \leq x < \infty$ .

The interference from the  $i$ -th CRT  $I_i$  can thus be written as

$$I_i = P_i |h_i|^2 r_i^{-\alpha}, \quad (2)$$

where  $r_i$  and  $P_i$  are respectively the distance from the PR to the  $i$ -th CRT, and the power of the  $i$ -th CRT. The aggregate interference  $I$  is

$$I = \sum_{i=1}^N I_i, \quad (3)$$

where  $N$  is the number of CRTs.

## III. INTERFERENCE ANALYSIS

This section derives the MGF and mean of  $I$  under three power control schemes, where  $I$  is the aggregate interference as introduced in the prior section.

The MGF of the aggregate interference is defined as  $M_I(s) = E[e^{-sI}]$ . Let  $M_{I_i}(s)$  define the MGF of the  $i$ -th CRT's interference. Because each interferer is independent, the MGF given  $N$  CRTs can be written as  $M_{I/N}(s) = (M_{I_i}(s))^N$ . Averaging with respect to the Poisson model (1) yields

$$M_I(s) = e^{\lambda_t A_t (M_{I_i}(s)-1)}, \quad (4)$$

where  $A_t = \pi (R_E^2 - R_G^2)$ .

Our objective now is to find  $M_{I_i}(s)$  under the different power control schemes.

### A. Scheme 1

This power control scheme is the simplest case. The CRT connects to the nearest CRR, and transmits at a power level to ensure a constant received power when averaged over small scale fading. This scheme is used extensively in the CDMA uplink to compensate the near-far problem [1], where all transmitters adjust their power such that the received power at the base station from each of them is the same.

Suppose  $P_c$  is the average received power<sup>1</sup> ensured, and  $r_c$  is the distance to the nearest CRR from the  $i$ -th CRT. Therefore, the transmit power level of the  $i$ -th CRT  $P_i = P_c r_c^\alpha$ .

Substituting  $P_i$  in (2), it is possible to write  $M_{I_i}(s)$  as

$$\begin{aligned} M_{I_i}(s) &= E_{|h_i|^2, r_i, r_c} [e^{-sI_i}] \\ &= E_{r_c} [E_{r_i} [E_{|h_i|^2} [e^{-sP_c r_c^\alpha r^{-\alpha} |h_i|^2}]]], \end{aligned} \quad (5)$$

due to the independence of  $|h_i|^2$ ,  $r_c$ , and  $r_i$ . After averaging with respect to  $|h_i|^2$ , we can obtain  $M_{I_i}(s)$  as

$$M_{I_i}(s) = E_{r_c} \left[ E_{r_i} \left[ \frac{1}{1 + sP_c r_c^\alpha r^{-\alpha}} \right] \right]. \quad (6)$$

However, when  $sP_c r_c^\alpha r^{-\alpha} < 1$ ,  $M_{I_i}(s)$  can be written as

$$M_{I_i}(s) = E_{r_c} \left[ E_{r_i} \left[ \sum_{t=0}^{\infty} (-sP_c r_c^\alpha r^{-\alpha})^t \right] \right]. \quad (7)$$

To evaluate this expectation, we require the distribution of  $r_i$ . Because a homogeneous PPP of CRTs was considered, the PDF of  $r_i$  can be obtained as

$$f_R(r_i) = \begin{cases} \frac{2\pi r_i}{A_t}, & R_G < r_i < R_E \\ 0, & \text{otherwise} \end{cases}. \quad (8)$$

We also require the distribution of the distance to the closest CRR from any given CRT ( $r_c$ ). Because the PPPs of CRRs and CRTs are independent, the location of any CRT is independent from the PPP of CRRs. Therefore,  $r_c$  is equivalent to the distance to the nearest node in a PPP from any given location, and follows the distribution [23]

$$f_{r_c}(x) = 2\pi\lambda_r x e^{-\pi\lambda_r x^2}, \quad 0 < x < \infty. \quad (9)$$

Averaging (7) with respect to  $r_i$  and  $r_c$  gives us

$$\begin{aligned} M_{I_i}(s) &= \frac{2\pi}{A_t} \sum_{t=0}^{\infty} (\pi\lambda_r)^{-\frac{\alpha t}{2}} (-sP_c)^t \left( \frac{R_E^{2-\alpha t} - R_G^{2-\alpha t}}{2 - \alpha t} \right) \\ &\times \Gamma\left(\frac{\alpha t}{2} + 1\right). \end{aligned} \quad (10)$$

From  $M_{I_i}(s)$ , we can find the moments of the aggregate interference in a straightforward manner. The mean aggregate interference  $E[I] = \lambda_t A_t E[I_i]$ , where  $E[I_i] = -\frac{d}{ds} M_{I_i}(s)|_{s=0}$ . Therefore,  $E[I]$  is found to be

$$E[I] = 2\pi\lambda_t P_c (\pi\lambda_r)^{-\frac{\alpha}{2}} \left( \frac{R_E^{2-\alpha} - R_G^{2-\alpha}}{2 - \alpha} \right) \Gamma\left(\frac{\alpha}{2} + 1\right). \quad (11)$$

<sup>1</sup>The average received power will be the receiver sensitivity plus an appropriate fade margin.

When  $\alpha = 2$ ,  $E[I]$  can be obtained after applying the L'Hospital's rule to (11) as

$$E[I]|_{\alpha=2} = \frac{4\pi\lambda_t P_c}{\pi\lambda_r} (\log(R_E) - \log(R_G)). \quad (12)$$

### B. Scheme 2

In the second scheme, while the CRT still has to ensure a constant average received power, there is an added constraint imposed by the primary system of a maximum allowable transmit power level  $P_s$ . If the required transmit power exceeds this threshold, cognitive transmission is aborted.

Now, the interference from the  $i$ -th transmitter (2) can be changed as  $I_i = Q_i P_i |h_i|^2 r_i^{-\alpha}$ , where  $Q_i$  is defined as follows:

$$Q_i = \begin{cases} 1, & P_i < P_s \\ 0, & \text{otherwise} \end{cases}.$$

Suppose  $q_i$  is the probability of  $P_i < P_s$ . Then,  $q_i = \Pr[P_c r_c^\alpha < P_s] = 1 - e^{-\pi\lambda_r \left(\frac{P_s}{P_c}\right)^{\frac{2}{\alpha}}}$ . We can now write

$$M_{I_i}(s) = E_{r_c} \left[ E_{r_i} \left[ 1 - q_i + \frac{q_i}{1 + sP_c r_c^\alpha r_i^{-\alpha}} \right] \right]. \quad (13)$$

By applying a series expansion, and averaging,  $M_{I_i}(s)$  becomes

$$\begin{aligned} M_{I_i}(s) &= 1 - q_i + q_i \sum_{t=0}^{\infty} (-sP_c)^t \left( \frac{2\pi}{A_t} \int_{R_G}^{R_E} r_i^{1-\alpha t} dr_i \right) \\ &\times \left( \frac{2\pi\lambda_r}{q_i} \int_0^{\left(\frac{P_s}{P_c}\right)^{\frac{1}{\alpha}}} r_c^{1+\alpha t} e^{-\pi\lambda_r r_c^2} dr_c \right) \\ &= e^{-\pi\lambda_r \left(\frac{P_s}{P_c}\right)^{\frac{2}{\alpha}}} + \frac{2\pi}{A_t} \sum_{t=0}^{\infty} \left( -\frac{sP_c}{\pi^{\frac{\alpha}{2}} \lambda_r^{\frac{\alpha}{2}}} \right)^t \left( \frac{R_E^{2-\alpha t} - R_G^{2-\alpha t}}{2 - \alpha t} \right) \\ &\times \left( \Gamma\left(\frac{\alpha t}{2} + 1\right) - \Gamma\left(\frac{\alpha t}{2} + 1, \pi\lambda_r \left(\frac{P_s}{P_c}\right)^{\frac{2}{\alpha}}\right) \right). \end{aligned} \quad (14)$$

Similar to Scheme 1, we can obtain  $E[I]$  as

$$\begin{aligned} E[I] &= 2\pi\lambda_t P_c (\pi\lambda_r)^{-\frac{\alpha}{2}} \left( \frac{R_E^{2-\alpha} - R_G^{2-\alpha}}{2 - \alpha} \right) \\ &\times \left( \Gamma\left(\frac{\alpha}{2} + 1\right) - \Gamma\left(\frac{\alpha}{2} + 1, \pi\lambda_r \left(\frac{P_s}{P_c}\right)^{\frac{2}{\alpha}}\right) \right). \end{aligned} \quad (15)$$

### C. Scheme 3

For the last power control scheme, we will go one step further from scheme 2 which assumes a constant maximum allowable transmit power  $P_s$ . We will now consider the case where it depends on  $r_i$  and  $\alpha$ . To minimize the PR interference, the CRTs close to the PR are given more stringent power requirements, and  $P_s$  becomes  $P_I r_i^\alpha$ , where  $P_I$  is a constant threshold value.

The probability of  $P_i < P_s$  ( $q_i$ ) would thus be  $1 - e^{-\pi\lambda_r r_i^2 \left(\frac{P_I}{P_c}\right)^{\frac{2}{\alpha}}}$ . By employing a similar method to the derivation of  $M_{I_i}(s)$  in Scheme 2, we can write  $M_{I_i}(s)$  for Scheme

3 as

$$M_{I_i}(s) = E_{r_i} \left[ e^{-\pi \lambda_r r_i^2 \left(\frac{P_I}{P_C}\right)^{\frac{2}{\alpha}}} + \sum_{t=0}^{\infty} \left( -\frac{s P_C}{\pi^{\frac{\alpha}{2}} \lambda_r^{\frac{\alpha}{2}}} \right)^t r_i^{-\alpha t} \right. \\ \left. \times \left( \Gamma\left(\frac{\alpha t}{2} + 1\right) - \Gamma\left(\frac{\alpha t}{2} + 1, \pi \lambda_r r_i^2 \left(\frac{P_I}{P_C}\right)^{\frac{2}{\alpha}}\right) \right) \right]. \quad (16)$$

After performing the expectation, the final equation for  $M_{I_i}(s)$  becomes (17), where  $\mathcal{W}(x, t)$  is given by (18).

The mean of the aggregate interference is found in a similar manner to the above schemes as

$$E[I] = \frac{2\pi \lambda_t P_C}{\pi^{\frac{\alpha}{2}} \lambda_r^{\frac{\alpha}{2}}} \left( \left( \frac{R_E^{2-\alpha} - R_G^{2-\alpha}}{2-\alpha} \right) \right. \\ \left. \times \Gamma\left(\frac{\alpha}{2} + 1\right) - (\mathcal{W}(R_E, 1) - \mathcal{W}(R_G, 1)) \right). \quad (19)$$

Moreover, the average probability of a CR being allowed to transmit  $q_i = 1 - \frac{2\pi}{A_t} \left( \frac{e^{-\pi \lambda_r \left(\frac{P_I}{P_C}\right)^{\frac{2}{\alpha}} R_G^2} - e^{-\pi \lambda_r \left(\frac{P_I}{P_C}\right)^{\frac{2}{\alpha}} R_E^2}}{2\pi \lambda_r \left(\frac{P_I}{P_C}\right)^{\frac{2}{\alpha}}} \right)$ .

#### IV. OUTAGE ANALYSIS

We will derive the CDF of the signal to interference and noise ratio (SINR) of the PR in this section. A simple variable substitution of the CDF gives the outage probability.

The primary transmitter is located at a distance  $R$  from the primary receiver, and has a power level of  $P_p$ . The primary signals are also assumed to undergo Rayleigh fading and path-loss. Therefore, the received power ( $P_R$ ) at the primary receiver can be written as

$$P_R = P_p R^{-\alpha} |h|^2, \quad (20)$$

where  $|h|^2$  is the channel power gain. Because a Rayleigh fading environment is assumed,  $|h|^2$  is exponentially distributed. Let  $\sigma_n^2$  denote the noise variance. The, SINR  $\gamma$  can be written as  $\gamma = \frac{P_p R^{-\alpha} |h|^2}{I + \sigma_n^2}$ . It is possible to obtain the CDF of the SINR as (see Appendix II for proof)

$$F_\gamma(x) = 1 - e^{\left(-\frac{x \sigma_n^2}{P_p R^{-\alpha}}\right)} M_I\left(\frac{x}{P_p R^{-\alpha}}\right). \quad (21)$$

Substituting the required threshold SINR ( $\gamma_{th}$ ) for  $x$  gives us the outage.

#### V. NUMERICAL RESULTS

This section shows the outage probability, mean aggregate interference, and the probability that CRTs are cut-off from transmission ( $1 - q_i$ ), under the different power control schemes. The best possible scheme would provide the CR network with the lowest average cut-off probability, while ensuring the PR has the lowest outage. We will use the parameters  $R_G = 20$ ,  $R_E = 100$ ,  $R = 30$ , and  $\gamma_{th} = 1$ . To highlight the effects of interference, and because interference is the prime inhibitor for our model, the additive noise variance  $\sigma_n^2$  is set to 0.

Fig. 2 plots the PR outage as a function of primary transmit power level  $P_p$  for scheme 3. The theoretical results match perfectly with the simulation. The outage reduces with respect

to  $P_p$  as expected. We see that the primary outage depends inversely with  $P_I$ . However, with regards to  $\alpha$ , the performance diminishes with its increase. Although we would expect that a higher  $\alpha$  would attenuate the interfering CR signals, it also means that the received primary power level is also low. Moreover, when  $\alpha$  is high, the transmit power of a CRT would also increase to ensure a constant average CRR received power ( $P_C$ ).

The PR outage vs the primary transmit power level  $P_p$  for Schemes 1 and 2 are plotted in Fig. 3. We observe that Scheme 1 results in the worst outage performance under a given CRR density ( $\lambda_r$ ). Furthermore, when  $\lambda_r$  increases, the PR's outage decreases because the distance between a CRT and its nearest CRR decreases, corresponding to a lower transmit CRT power level. Therefore, to increase the PR's outage performance on a practical standpoint, the CR network needs to have a sufficient cut-off power level, and the CRR density needs to be sufficiently high.

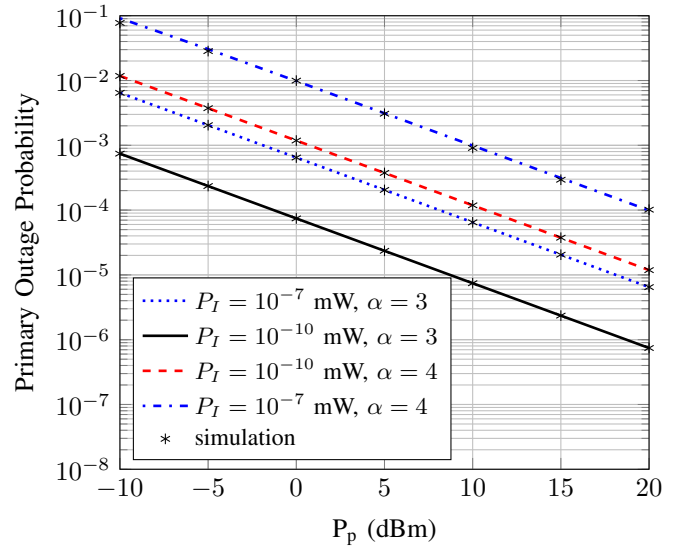


Fig. 2: Scheme 3: The PR outage probability vs the primary power level  $P_p$  for different values of  $P_I$ , and  $\alpha$ .  $\lambda_t = 5 \times 10^{-3}$ ,  $P_C = 10^{-8}$  mW, and  $\lambda_r = 2.5 \times 10^{-3}$ .

The primary outage probability under Scheme 2 is plotted over the CRT cut-off power threshold  $P_s$  in Fig. 4. Naturally, we would expect the outage to increase as  $P_s$  increases. However, the outage increases initially, and then flattens out. This is because at higher cut-off levels, almost all the CRT transmit powers would fall below the threshold. Moreover, the rate of outage increase before flattening out depends on the CRR density  $\lambda_r$ . The CRT density  $\lambda_t$  only introduces a shift to the curves, and does not affect the shape.

Fig. 5 plots the mean aggregate interference power under all 3 schemes with respect to the average received power level of a CRR ( $P_C$ ). As expected, Scheme 1 provides the worst interference, and shows a constant increase with respect to  $P_C$ . However, for Schemes 2 and 3, there exists a maxima when the mean interference is at its highest. For these two

$$M_{I_i}(s) = \frac{2\pi \left( \frac{e^{-\pi\lambda_r \left(\frac{P_I}{P_c}\right)^{\frac{2}{\alpha}} R_G^2} - e^{-\pi\lambda_r \left(\frac{P_I}{P_c}\right)^{\frac{2}{\alpha}} R_E^2}}{2\pi\lambda_r \left(\frac{P_I}{P_c}\right)^{\frac{2}{\alpha}}} + \sum_{t=0}^{\infty} \left( \frac{s P_c}{\pi^{\frac{\alpha}{2}} \lambda_r^{\frac{\alpha}{2}}} \right)^t \left( \frac{R_E^{2-\alpha t} - R_G^{2-\alpha t}}{2-\alpha t} \right) \Gamma\left(\frac{\alpha t}{2} + 1\right) - (\mathcal{W}(R_E, t) - \mathcal{W}(R_G, t)) \right)}{A_t} \quad (17)$$

$$\mathcal{W}(x, t) = \frac{e^{-\pi\lambda_r x^2 \left(\frac{P_I}{P_c}\right)^{\frac{2}{\alpha}}}}{\alpha t - 2} \left( (\pi\lambda_r)^{\frac{\alpha t}{2} - 1} \left(\frac{P_I}{P_c}\right)^{t - \frac{2}{\alpha}} \left( \pi\lambda_r x^2 \left(\frac{P_I}{P_c}\right)^{\frac{2}{\alpha}} + 1 \right) - x^{2-\alpha t} e^{\pi\lambda_r x^2 \left(\frac{P_I}{P_c}\right)^{\frac{2}{\alpha}}} \Gamma\left(\frac{\alpha t}{2} + 1, \pi\lambda_r x^2 \left(\frac{P_I}{P_c}\right)^{\frac{2}{\alpha}}\right) \right) \quad (18)$$

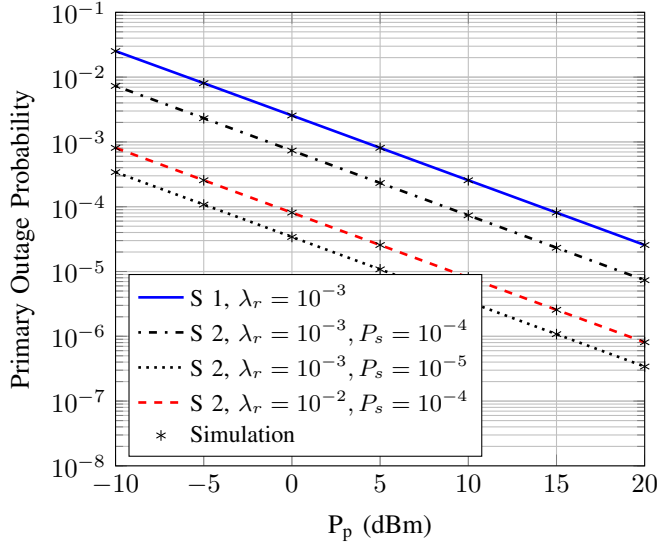


Fig. 3: Schemes 1 and 2: The outage probability vs the primary power level  $P_p$  for different values of  $P_s$ , and  $\lambda_r$ .  $\lambda_t = 5 \times 10^{-3}$ ,  $P_c = 1 \times 10^{-8}$ , and  $\alpha = 3$ .

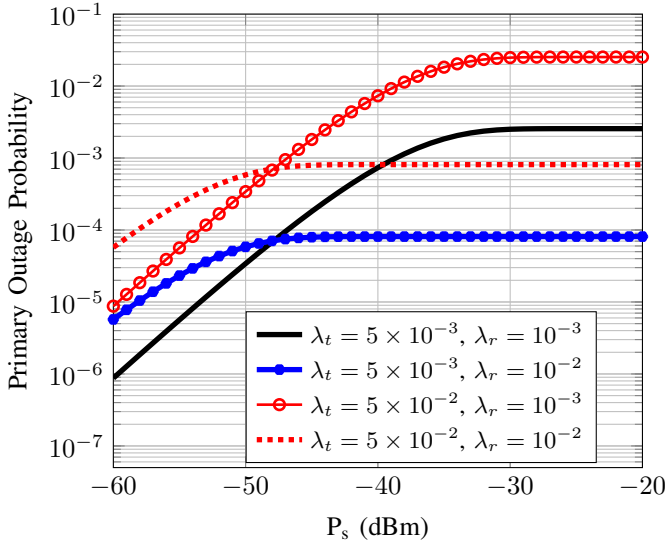


Fig. 4: Scheme 2: The PR outage probability vs the cut-off threshold  $P_s$  for different values of  $\lambda_t$ , and  $\lambda_r$ .  $\alpha = 3$ ,  $P_p = 1$  mW, and  $P_c = 10^{-8}$  mW.

schemes, when the average received CRR power is low, the transmit powers of the CRTs are low, and thus results in a low interference. When  $P_c$  increases, the CRT transmit powers would increase, and in turn the interference would increase.

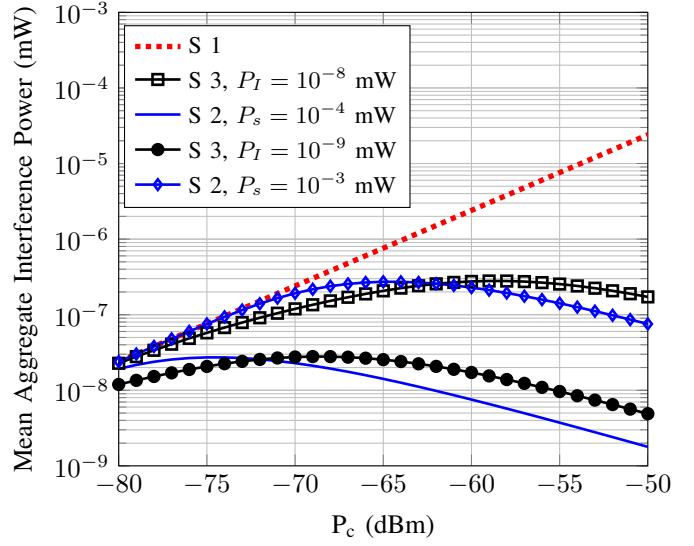


Fig. 5: The mean aggregate interference vs the average received CR power  $P_c$  for the 3 schemes, under different  $P_s$  and  $P_I$ .  $\alpha = 3$ ,  $\lambda_t = 5 \times 10^{-3}$ , and  $\lambda_r = 2.5 \times 10^{-3}$ .

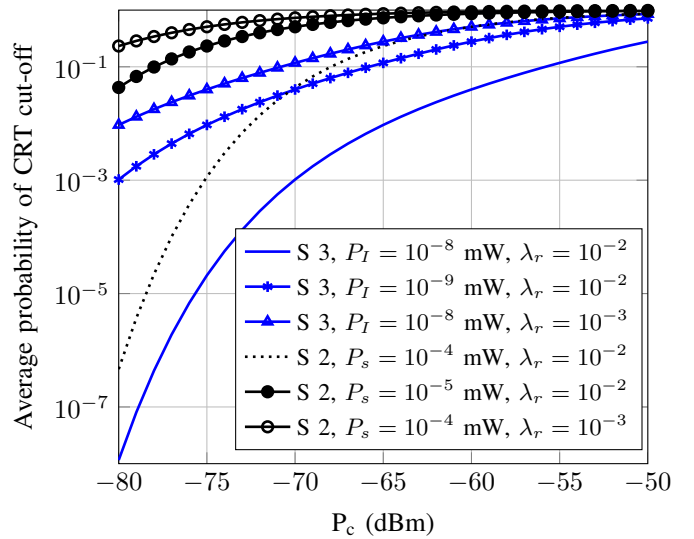


Fig. 6: The average probability of a CRT being cut-off from transmission ( $E[1 - q_i]$ ) vs  $P_c$  for Schemes 2 and 3, under different  $\lambda_r$ ,  $P_s$ , and  $P_I$ .  $\alpha = 3$ .

However, as  $P_c$  increases even further, the number of CRTs getting cut-off due to having a transmit power greater than the cut-off level  $P_s$  would increase. Therefore, this reduction in transmitting CRTs leads to a lower aggregate interference, and thus the maxima occurs. The value of  $P_c$  when the maxima

occurs is dependent on several factors, and can be obtained through differentiation by using the derived equations for  $E[I]$ . Moreover, as  $P_c$  increases, Scheme 3 can generate a slightly higher mean aggregate interference to the PR, whereas the opposite is true for lower  $P_c$ .

It is important to gain an understanding on the impact of different power control schemes on the cognitive system. Fig. 6 plots the probability that a CRT is cut-off from transmitting with respect to the average received CRR power  $P_c$ , for Schemes 2 and 3. For Scheme 1, this probability is 0. For a high CRR density  $\lambda_r$ , the curves show a sharp drop-off under higher  $P_s$  or  $P_I$  when  $P_c$  is low. Furthermore, as  $P_c$  reduces, the drop-off for Scheme 2 is higher than Scheme 3, corresponding to a better availability for the CR network. To conclude, a high CRR density, a low average received CRR power  $P_c$ , and a higher value for the thresholds  $P_s$  or  $P_I$  (corresponding to Scheme 2 and 3 respectively) reduces the probability that a CRT is cut-off from transmitting.

## VI. CONCLUSION

This paper has investigated the aggregate interference power of an annular underlay CR network in which CRTs and CRRs are spatially distributed as independent PPPs. Each CRT transmits to the closest CRR. Three different transmit power control schemes, based on: 1) CR transmitter-receiver distance  $r_c$  2)  $r_c$  and a constant cut-off power level 3)  $r_c$  and a random cut-off power level, have been considered. The MGF and mean of the aggregate interference, and the PR outage probability have been derived. It has been shown that the CR transmission/receiver thresholds and the CRR density significantly impact the primary performance. For Schemes 2 and 3, there also exists a worst case average received power for a CRR when the mean interference peaks. Furthermore, it was shown that Scheme 1 which allows all the CRTs to communicate with their respective receivers provides the worst PR performance. Future research directions include considering CR transmissions to multiple receivers, and investigation of channel state information-assisted power control schemes.

### APPENDIX I :PROOF OF CDF $F_\gamma(x)$

$$F_\gamma(x) = \Pr[\gamma \leq x].$$

We can write

$$\begin{aligned} F_{\gamma/I}(x) &= \Pr \left[ \frac{P_p R^{-\alpha} |h|^2}{I + \sigma_n^2} \leq x \right] \\ &= \Pr \left[ |h|^2 \leq \frac{x(I + \sigma_n^2)}{P_p R^{-\alpha}} \right] \\ &= 1 - e \left( -\frac{x(I + \sigma_n^2)}{P_p R^{-\alpha}} \right). \end{aligned}$$

After averaging with respect to  $I$ , we obtain

$$\begin{aligned} F_\gamma(x) &= 1 - e \left( -\frac{x\sigma_n^2}{P_p R^{-\alpha}} \right) E_I \left[ e^{-I \left( \frac{x}{P_p R^{-\alpha}} \right)} \right] \\ &= 1 - e \left( -\frac{x\sigma_n^2}{P_p R^{-\alpha}} \right) M_I \left( \frac{x}{P_p R^{-\alpha}} \right), \end{aligned}$$

which is equation (21).

## REFERENCES

- [1] A. Molisch, *Wireless Communications*. Wiley-IEEE Press, 2011.
- [2] P. Mach and Z. Becvar, "QoS-guaranteed power control mechanism based on the frame utilization for femtocells," *EURASIP Journal on Wireless Communications and Networking*, vol. 2011, 2011.
- [3] J. Jang and K.-B. Lee, "Transmit power adaptation for multiuser OFDM systems," *IEEE J. Sel. Areas Commun.*, vol. 21, no. 2, pp. 171–178, 2003.
- [4] D. Qiao, S. Choi, and K. Shin, "Interference analysis and transmit power control in IEEE 802.11a/h wireless LANs," *IEEE/ACM Trans. Networking*, vol. 15, no. 5, pp. 1007–1020, 2007.
- [5] S. Gong, P. Wang, Y. Liu, and W. Zhuang, "Robust power control with distribution uncertainty in cognitive radio networks," *IEEE J. Sel. Areas Commun.*, vol. 31, no. 11, pp. 2397–2408, 2013.
- [6] C. Sun, Y. Alemseged, H.-N. Tran, and H. Harada, "Transmit power control for cognitive radio over a Rayleigh fading channel," *IEEE Trans. Veh. Technol.*, vol. 59, no. 4, pp. 1847–1857, 2010.
- [7] S. Srinivasa and S. Jafar, "Cognitive radios for dynamic spectrum access - the throughput potential of cognitive radio: A theoretical perspective," *IEEE Commun. Mag.*, vol. 45, no. 5, pp. 73–79, May 2007.
- [8] S. Hu, Y.-D. Yao, and Z. Yang, "Mac protocol identification approach for implement smart cognitive radio," in *Proc. IEEE ICC*, 2012, pp. 5608–5612.
- [9] A. Goldsmith, S. Jafar, I. Maric, and S. Srinivasa, "Breaking spectrum gridlock with cognitive radios: An information theoretic perspective," *Proc. IEEE*, vol. 97, no. 5, pp. 894–914, 2009.
- [10] A. Rabbachin, T. Q. S. Quek, H. Shin, and M. Z. Win, "Cognitive network interference," *IEEE J. Sel. Areas Commun.*, vol. 29, no. 2, pp. 480–493, Feb. 2011.
- [11] L. Vijayandran, P. Dharmawansa, T. Ekman, and C. Tellambura, "Analysis of aggregate interference and primary system performance in finite area cognitive radio networks," *IEEE Trans. Commun.*, vol. PP, no. 99, pp. 1–12, 2012.
- [12] A. Babaei and B. Jabbari, "Interference modeling and avoidance in spectrum underlay cognitive wireless networks," in *Proc. IEEE ICC*, May 2010, pp. 1–5.
- [13] S. Kusaladharna and C. Tellambura, "On approximating the cognitive radio aggregate interference," *IEEE Wireless Commun. Lett.*, vol. 2, no. 1, pp. 58–61, 2013.
- [14] M. J. Rahman and X. Wang, "Probabilistic analysis of mutual interference in cognitive radio communications," in *Proc. IEEE GLOBECOM*, Dec. 2011, pp. 1–5.
- [15] S. Kusaladharna and C. Tellambura, "Aggregate interference analysis for underlay cognitive radio networks," *IEEE Wireless Commun. Lett.*, vol. 1, no. 6, pp. 641–644, 2012.
- [16] M. Hanif, M. Shafi, P. Smith, and P. Dmochowski, "Interference and deployment issues for cognitive radio systems in shadowing environments," in *Proc. IEEE ICC*, Jun. 2009, pp. 1–6.
- [17] X. Hong, C.-X. Wang, and J. Thompson, "Interference modeling of cognitive radio networks," in *Proc. IEEE VTC*, May 2008, pp. 1851–1855.
- [18] Z. Chen, C.-X. Wang, X. Hong, J. Thompson, S. Vorobyov, X. Ge, H. Xiao, and F. Zhao, "Aggregate interference modeling in cognitive radio networks with power and contention control," *IEEE Trans. Commun.*, vol. 60, no. 2, pp. 456–468, Feb. 2012.
- [19] J. F. Kingman, *Poisson Processes*. Oxford University Press, 1993.
- [20] I. Gradshteyn and I. Ryzhik, *Table of integrals, Series, and Products*, 7th ed. Academic Press, 2007.
- [21] P. C. Pinto and M. Z. Win, "Communication in a Poisson field of interferers—part I: Interference distribution and error probability," *IEEE Trans. Wireless Commun.*, vol. 9, no. 7, pp. 2176–2186, Jul. 2010.
- [22] E. Salbaroli and A. Zanella, "Interference analysis in a Poisson field of nodes of finite area," *IEEE Trans. Veh. Technol.*, vol. 58, no. 4, pp. 1776–1783, May 2009.
- [23] D. Stoyan, W. S. Stoyan, Kendall, and J. Mecke, *Stochastic Geometry and its Applications*. John Wiley & Sons Ltd., 1995.
- [24] J. Andrews, F. Baccelli, and R. Ganti, "A tractable approach to coverage and rate in cellular networks," *IEEE Trans. Commun.*, vol. 59, no. 11, pp. 3122–3134, 2011.
- [25] A. Goldsmith, *Wireless Communications*. Cambridge University Press, 2005.